Journal of Innovative Optical Health Sciences
Vol. 12, No. 1 (2019) 1841004 (8 pages)

DOI: 10.1142/S1793545818410043

Characterizing the luminescent properties of upconversion nanoparticles in single and densely packed state

Xiaohu Chen*,‖, Zhengyu Gui*,§,‖, Yong Liang*, Xin Jin*, Simin Li*, Pengjiu Zhao*, Zhangsen Yu†, Aiguo Wu†, Shoupeng Liu‡ and Hui Li*,¶

*Jiangsu Key Laboratory of Medical Optics
CAS Center for Excellence in Molecular Cell Science
Suzhou Institute of Biomedical Engineering and Technology
Chinese Academy of Sciences, Suzhou 215163, P. R. China

†Key Laboratory of Magnetic Materials and
Devices & Functional Materials and Nanodevices
Ningbo Institute of Material Technology & Engineering
Chinese Academy of Sciences Ningbo 315201, P. R. China

‡Tianjin Guoke Medical Engineering and Technology
Development Co., Ltd., Tianjin 300399, P. R. China

§Jiangsu Shuguang Opto-Electronics Co., Ltd., Yangzhou 225009, P. R. China
¶Hui.li@sibet.ac.cn

Received 26 November 2018
Accepted 9 January 2019
Published 15 February 2019

Luminescent properties of Er^{3+}- and Yb^{3+}- co-doped CaF_2 upconversion nanoparticles (UCNPs) were investigated in single particle and densely-packed states with a custom-built microscope. The single UCNPs exhibit linear dependency of luminescent intensity on excitation power while the densely-packed UCNPs exhibit a 2-order power law-dependency indicating a two-photon absorption process. Time-domain luminescence intensity measurements were performed and the curves were fitted to excitation\emission rate functions based on a simplified three-state model. The results indicate that the intermediates in single particles are much less and saturated in a short time, and there are strong couplings of the ground states and intermediate states between neighboring UCNPs in densely packed UCNPs.

Keywords: Upconversion nanoparticles; single particles; luminescence; lifetime; rate function.

¶Corresponding author.
‖These two authors contributed equally to this study.

1. Introduction

Photon upconversion (UC) is a process in which the sequential absorption of two or more photons leads to the emission of light at a shorter wavelength than the excitation,[1,2] such as the conversion of infrared light to visible light. Upconversion nanoparticles (UCNPs) received much attention in recent years for their potential application in biomedical imaging, cancer diagnosis, and therapy. Higher penetration depth, low auto-fluorescence and minimized photo-damage made the UCNPs a promising alternative probe to molecular fluorophore for biomedical imaging of cells, tissue, and even live animals.[3–7]

In contrast to traditional two-photon absorption/emission process, a long-lived intermediate state usually exists in UCNPs which greatly increases the quantum efficiency. Hence, a low-peak-power continuous laser could be used to excite the UCNPs for scanning microscopy instead of expensive femtosecond pulse laser.[8,9] In 2009, Yu *et al.* reported laser scanning upconversion luminescence microscopy (LSUCLM) with a confocal pinhole for 3D section imaging.[9] In 2015, Hodak *et al.* found that nonlinear dependence of luminescent intensity on excitation power could be realized using pulse excitation.[8] By adjusting power and excitation rate, optical sectioning similar to traditional two-photon microscope was achieved.[8] However, the nonlinearity was obtained on the relative dense sample. For application in cell biology, mostly the sample needs to be labeled with a low concentration of UCNPs yielding a single particle state. So characterizing the luminescent properties of UCNPs is demanded.

So far, luminescence properties of UCNPs were characterized mostly in ensemble measurement. To increase the photon efficiency of UCNPs by optimizing the synthesis strategies, i.e., changing the morphology, size, doping ions etc,[10,11] ensemble measurements are sufficient. But the underlying UC mechanism could be averaged out with a large number of particles.[12] To recover that, measurements need to be done at single particle level.[13] In 2014, Gargas *et al.* characterized sub-10 nm upconverting nano-crystals for single-molecule imaging.[14] However, its UC process and the difference to bulk samples is still not clear.

In this paper, luminescent properties of single and densely packed UCNPs were studied with a custom-built laser scanning microscope. The dependency of the luminescent intensity of excitation laser power and time domain luminescent measurement demonstrates a single-photon adsorption process due to saturation of the intermediate state for single UCNPs. But a two-photon adsorption and a continuous luminescent increase even after turning off the excitation laser power was observed for densely packed UCNPs. The results suggest more intermediate states and excitation and decay pathways between neighboring particles exist in the densely packed sample.

2. Materials and Methods

Previously synthesized Er^{3+} and Yb^{3+} co-doped CaF_2 UCNPs were stored as dried powder. A 10 mg powder was suspended in 1 ml cyclohexane and shaken gently by hand. For the densely packed sample, 1 drop of 10 μl sample was spread on freshly cleaned coverslip. For the sparsely dispersed single particle sample, the solution was further diluted 10,000x with cyclohexane and sonicated for 5 min, then 1 drop of 10 μl sample was spread on a freshly cleaned coverslip. Both samples were dried in air. 10 μl water was dipped on the sample surface before mounting on the microscope.

A previously custom-built microscope was modified slightly to measure the UCNPs' luminescence properties,[15] as shown in Fig. 1 Briefly, a 980 nm laser was used as excitation light source and a pockels-cell was used to turn on/off the light with sub μs time resolution. The laser beam was raster scanned by a pair of Galvo mirrors and guided into objective by a scan lens and a tube lens. A 60 × water-immersion objective (Nikon Plan Apo VC 60 ×) was used for imaging and collecting emitted luminescence. The luminescent signal was separated from excitation laser by a dichroic mirror and further cleaned by a band-pass filter. A PMT detector and a spectrometer were used to detect the intensity and measure the spectrum, respectively, switched by a flipper mirror.

The microscope can work at three different modes: spectrum recording mode, scan imaging mode and time domain luminescent intensity measuring mode. When working at spectrum recording mode, the Galvo-mirrors remain at a fixed position and the flipper mirror was flipped up to guide the luminescent light into the spectrum. While working at scan imaging mode, the luminescent intensity was detected by the PMT with the Galvo-mirror raster-scanning the sample to record the 2D image.

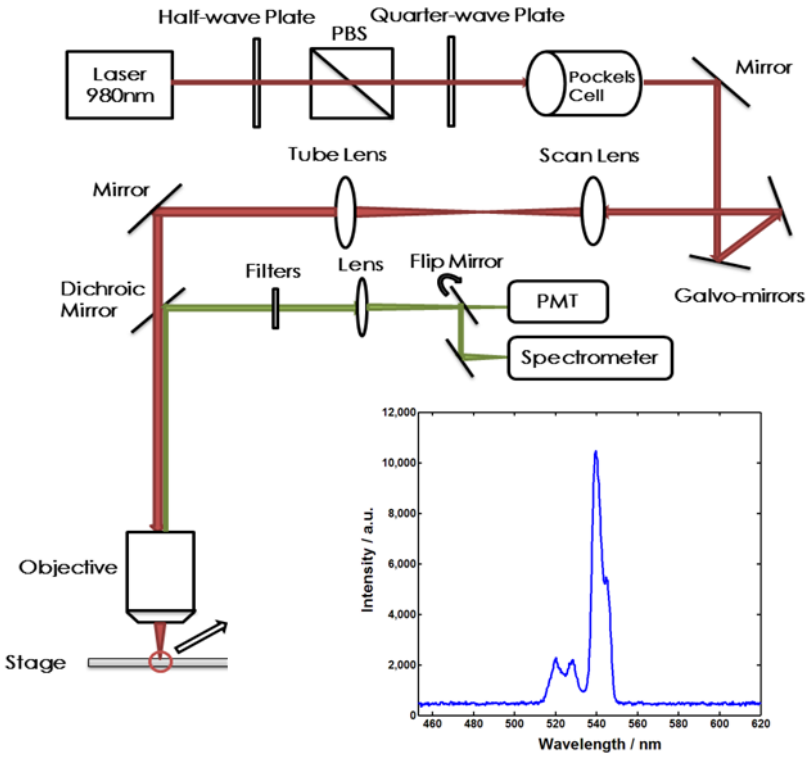

Fig. 1. Sketch of the custom-built microscope for measuring the luminescence properties of UCNPs. The inset shows the measured luminescence spectrum of Er3+ and Yb3+ co-doped CaF_2 UCNPs.

Once the t image was recorded, points of interesting could be selected by hand, then the Galvo-mirror stopped the scan and kept at these positions one by one iteratively to record the time-domain luminescent intensity. At each position, the excitation laser was turned on by the electro-optic modulating pockels-cell for a short period of time, generally 500 μs, and the luminescent intensity was recorded continuously until decay to zero.

3. Results and Discussion

3.1. *Spectrum of UCNPs particles*

Densely packed UCNPs sample was prepared by drying high concentration suspension on coverslip. When excited by 980 nm laser with 1 mW laser intensity, strong luminescence could be seen by naked eyes. The measured spectrum is shown in the inset of Fig. 1. The spectrum is ranged from 514 nm to 550 nm with maximum intensity at 541 nm. There are another two weak emission peaks at 520 nm and 532 nm, respectively. This 550 band belong to $^4S_{3/2}$ to $^4I_{15/2}$ which is more suitable for kinetic studies.[8] It is known that UCNPs has another emission band at 660 nm, which corresponds to $(^4F_{9/2} - {}^4F_{15/2})$, which is blocked by the dichroic mirror in our system.[15] In the following experiment, one addition band-pass filter (500–560 nm) was used to further clean the luminescent signal. With the same excitation laser intensity, the luminescent signal is too strong to be recorded by a PMT detector. So, in the following experiment, the detection of densely packed UCNPs sample was all done with the spectrometer.

3.2. *Imaging UCNPs in single particle state*

Single UCNPs sample was prepared by diluting the suspension 10,000× times and then drying on coverslip. The excitation laser was scanned across the sample by Galvo-mirrors and the luminescence intensity was detected by PMT. Figure 2 shows the luminescence image with different scanning speed. With a slow scanning speed of 50 lines/s, corresponding to 40 μs dwell time for each pixel, most spheres can be clearly distinguished and have a round shape which verified the sparely dispersed single particle states. However, at fast scanning speed, the spheres appear to be elongated. The

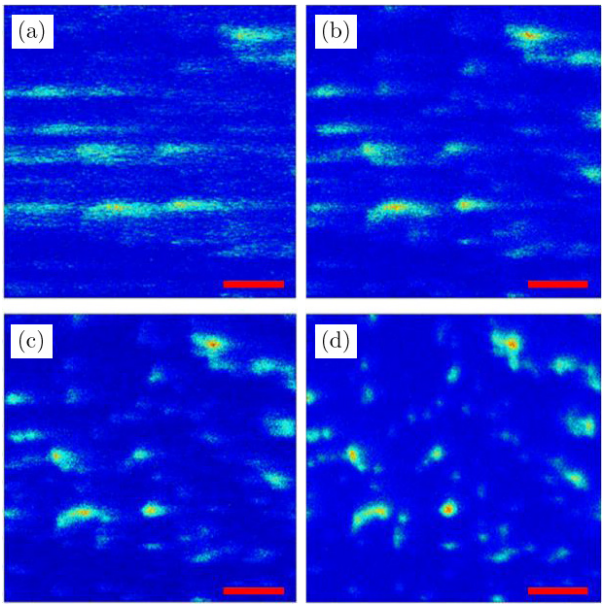

Fig. 2. Luminescent image of sparsely dispersed UCNPs at different scanning speed: (a) 2 μs per pixel, (b) 5 μs per pixel, (c) 10 μs per pixel, (d) 40 μs per pixel. Scale bar represents 2 μm.

particles were elongated more and more with increased speed, i.e., shorter of dwell time.

The elongation at fast velocity was not due to the scanning mechanics of the microscope since the peak positions of each particle remain the same with different velocities. We hypothesize that they were due to the long lifetime of UCNPs. Since the microscope was working at nondescan mode, there was no pinhole used to reject the luminescent signal out of the excitation focus spot. In case of luminescence lifetime longer than the pixel dwell time, the excited UCNPs continue to emit luminescence even after the laser beam was scanned to the next pixel position. As a result, in the 2D image construction, the luminescence was also contributed to the next pixel position, hence the image was elongated. In order to avoid smearing, accurate imaging of single-particle UCNPs requires a slower scanning speed. In the following, a scanning speed with a dwell time of 40 μs was used.

3.3. *Dependence of luminescent intensity on excitation power*

Next, we measured the luminescent intensity dependence on excitation power. For sparsely dispersed single particles, the sample was imaged at low scanning speed (40 μs pixel dwell time) with different excitation laser power ranging from 100 to 1400 μW. The intensity of each UCNP was calculated as the sum of a 13-pixel area around the particle after subtracting background. Figure 3(a) shows a plot of a typical UCNP which demonstrates a nearly-linear dependency. For the densely packed sample, the luminescent intensity at the peak of 545 nm read from the spectrometer while varying the excitation laser power. On the contrary to single UCNPs, a nonlinear dependency is clearly seen for densely packed UCNPs as plotted in Fig. 3(b).

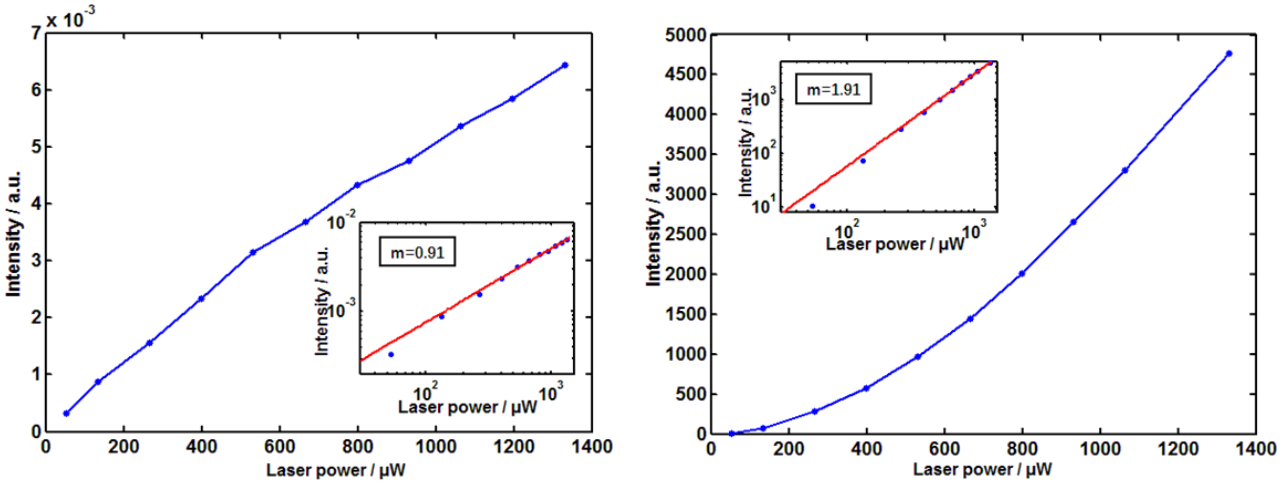

(a) (b)

Fig. 3. Dependence of the luminescent intensity on excitation laser power for a single UCNP (a) and densely packed sample (b). Insets show the corresponding log–log plot.

Generally, the dependence of luminescence intensity on excitation power can be described by a power-law equation[3]:

$$I_{\mathrm{UCNPs}} \propto P^m, \tag{1}$$

where I_{UCNPs} represents the luminescent intensity, P represents the excitation power, and m represents the absorption coefficient which is 1 for single-photon absorption and 2 for two-photon absorption process.

Insets of Fig. 3 show the log–log plot of the luminescent intensity dependent on the excitation power. By fitting the log–log plot with a linear function, the slop represents the absorption coefficient m. The absorption coefficients of 0.91 and 1.91 were obtained for single UCNPs and densely packed UCNPs, respectively. The absorption coefficients are not integer but fractional indicating complex process were involved during the UC. But it is clearly demonstrated that the single UCNPs undergo a more-or-less one-photon absorption process while densely packed UCNPs undergo a two-photon absorption process with the same 980 nm laser excitation.

The different dependency between single and densely packed UCNPs can be explained by the saturation of the intermediate state. Different to general two-photon absorption with a femtosecond laser, one or more real long-lived intermediate states exist as energy reservoirs in the UC process. Upon absorption of the first photon, the particles undergo a transition from ground state to the intermediate state, stay there for up to hundreds of μs until absorption of the second photon or decay back to ground state. Upon absorption of the second photon by either excited state absorption (ESA) or energy transfer up-conversion (ETU) process, the particles transit from intermediate to the excited stated and are capable of emitting luminescence. For single UCNPs, although the particles need to absorb two photons to emit luminescence, the long-lived intermediate states prevent its decay to ground state before absorption of the second photon. In other words, the intermediate state always remains saturated upon the photon flux, so the dependence of the luminescent intensity on excitation power will only represent the transition process from intermediate state to excited state. Hence, a single-photon absorption behavior was observed as shown in Fig. 3(a). On the contrary, the absorption coefficient of 1.91 in Fig. 3(b) suggests that intermediate state is not saturated in densely packed UCNPs in the same range of excitation power. This could be due to more intermediate states or more decay pathways from the intermediate state to ground state for densely packed UCNCPs.

3.4. *Time-domain luminescent intensity measurement*

We further characterize the UC and luminescence process by time-domain measurement. Briefly, positions of each identified single particle were obtained from the image with low scanning speed. Then the excitation laser was turned off and scan mirrors were kept at each position successively so that the laser beam was focused on the particle for a certain period of time until the measurement is finished. At each position, a function generator generates a 500 μs pulse to turn on the laser and trigger the acquisition of luminescent intensity simultaneously. For the densely packed sample, the same measurements were performed except that the focus position does not need to be changed. Figure 4 shows typical time-domain luminescent intensity curves for single UCNPs and densely packed sample.

The curves constitute two regions, the first 500 μs region corresponds to UC with excitation laser on; the rest corresponds to luminescent decay with laser off. In the laser-off region, both samples exhibit single exponential decay although the decay time of a single particle is much shorter than the densely packed sample. The laser-on region is more complicated because it may involve a few photon absorptions and emission pathway at the same time. For single particles, the luminescent intensity first undergoes a fast increase ($< 100\,\mu$s) then slowly reaches a plateau which suggests the saturation of excited states. For the densely packed sample, the luminescent intensity increased slowly at the beginning ($< 30\,\mu$s) then continually increased in a nearly-linear behavior. Interestingly, even after the excitation laser was turned off, the luminescent intensity still increased for about 20 μs for the densely packed sample, as shown in the inset of Fig. 4.

3.5. *Upconversion model for single and densely packed UCNPs*

In the above experiment, differents absorption coefficients and different time-domain luminescent behavior for single and densely packed UCNPs were observed. Gamelin and Gudel developed a simplified three-state model to simulate the process.[16]

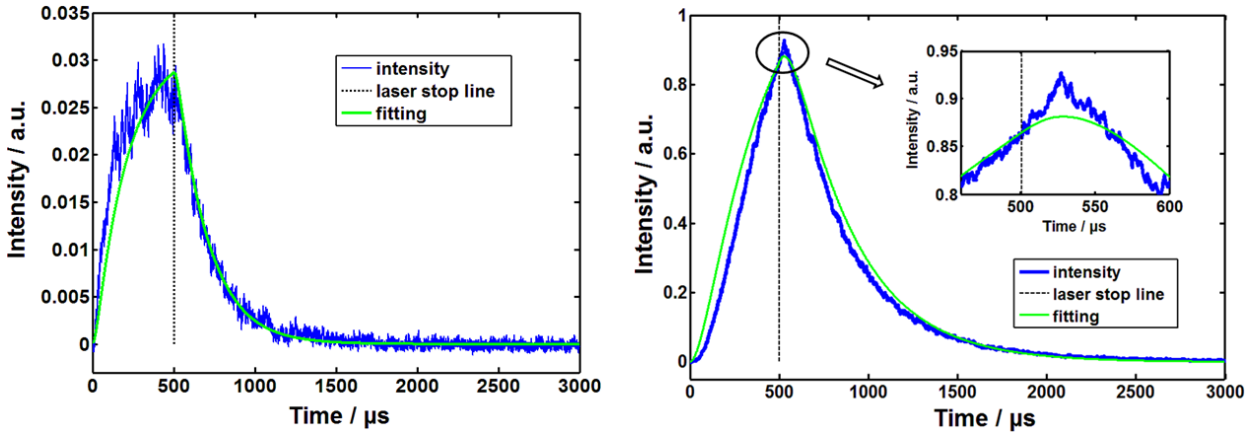

Fig. 4. Time domain luminescence intensity for single UCNP (a) and densely packed UCNPs (b).

We used the same model to describe the difference between single and densely packed UCNPs. Figure 5(a) shows the scheme of the electron state distribution of Er^{3+}-Yb^{3+} co-doped UCNPs. Er^{3+} at the shell first absorb one 980 nm photon and transit the molecule from ground state S_0 to intermediate state S_1. The energy can be transferred to the first excited state of Yb^{3+}. Upon adsorption of the second photon, the particle was transited to emissive state S_2 from excited states S_1. N_0, N_1 and N_2 denote the populations of the ground (S_0), intermediate (S_1) and emissive (S_2) states, then the absorption and emission process can be described as following equations[8]:

$$\frac{dN_0}{dt} = -GN_0 + k_1N_1 + k_2N_2, \tag{2}$$

$$\frac{dN_1}{dt} = GN_0 - k_1N_1 - EN_1, \tag{3}$$

$$\frac{dN_2}{dt} = EN_1 - k_2N_2, \tag{4}$$

where G is the ground state excitation rate constant, k_1 and k_2 are the decay constant from the intermediate state and the emissive state to ground state, respectively, E is the excited state excitation rate constant, by which absorption of the second photon can excite the particle from intermediate state S_1 state to emissive state S_2. The luminescent intensity is proportional to the population of the emissive state and the decay rate from emissive state to ground state, i.e., $(k_2 \times N_2)$.

Time-domain luminescent intensity curves in Figs. 4(a) and 4(b) were fitted to above function using the ode45 method. Table 1 lists the parameters of best fitting results to single and densely packed UCNPs. The results show that G of densely packed UCNPs are 30 times larger than that of single particles, which suggests a strong cooperative absorption between neighboring particles in the densely packed sample. Because the ground states

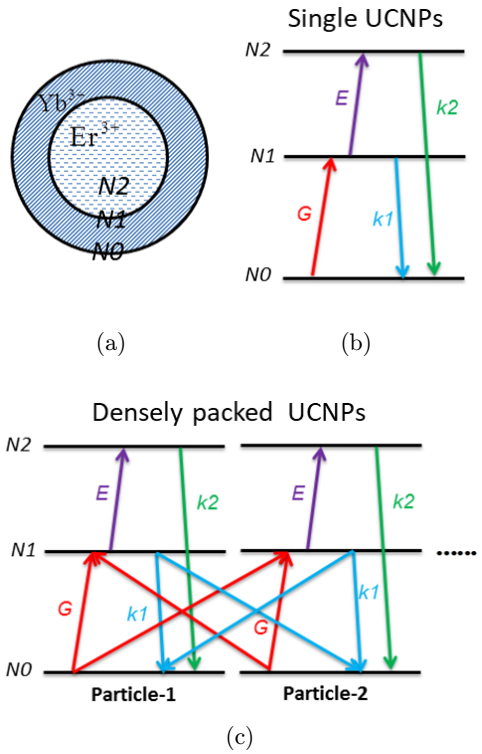

Fig. 5. Scheme of the electron state distribution of the UCNP (a), and the excitation and emission process for a single (b) and densely packed UCNPs (c).

Table 1. Fitting of time domain luminescent intensity of single and densely packed UCNPs to a three-state model.

Sample type	G_0 (s^{-1})	E (s^{-1})	k_1 (s^{-1})	k_2 (s^{-1})
Single	1	0.41	1.5×10^4	2.8×10^3
Densely packed	30	0.4	5×10^4	5.1×10^3

are mostly distributed in the shell, there are possible excitations from the ground of one particle to the intermediate states of neighboring particles. However, the ETU rate constant E is about the same. This is because both the intermediate and the emissive states are mostly distributed in the core, hence there is less possibility of excitation from an intermediate state of one particle to the emissive state of another particle. The results also show that both the decay constants k_1 and k_2 of densely packed UCNPs are 2–3 times larger than that of single UCNPs, indicating multiple decay pathways exist for the former since it is possible from the intermediate and emissive state of one particle to the ground state of nearly other particles, as illustrated in Fig. 5(c).

The continual luminescent intensity increase after excitation laser is turned off is also presented in the fitted data for densely packed UCNPs, as shown in the inset of Fig. 4(b). This can be explained as that there are enough electrons at the long-life intermediate state, $E \times N_1$ is still larger than $k_2 \times N_2$ which leads to the electrons at the emissive state still increasing even when the excitation laser is powered off during this short 20 μs period. This phenomenon was not observed in single UCNPs indicating that the number of intermediate states is much lesser than compared to densely packed sample. So even the excitation rate constant G_0 is small for the intermediate state which is more likely to be saturated.

4. Conclusions

With a custom-built scanning microscope, luminescent properties of single and densely packed UCNPs were studied. Both luminescence-excitation dependency and the time-domain luminescent measurement suggests saturation of intermediate state for single UCNPs which leads to one-photon adsorption behavior. However, same measurements on densely packed UCNPs suggest that more intermediate states exist as well as more excitation and decay pathways between neighboring particles, which leads to two-photon adsorption behavior and increased excitation and decay rate constant. The very different luminescent properties of single UCNPs to densely packed ones will affect the experiment design and obtained results for its application in biomedical imaging.

Acknowledgments

The work was supported by the National Key Research and Development Program of China (YFC20170110100), the National Natural Science Foundation of China (NSFC) (Grant Nos. 61475185 and 11504409), and Natural Science Foundation of Tianjin City (TJNSF) (Grant No. 16JCYBJC43800). Xiaohu Chen and Zhengyu Gui contributed equality to this work.

References

1. F. Auzel, "Upconversion and anti-stokes processes with f and d lons in solids," *Chem. Rev.* **104**(1), 139–173 (2004).
2. Q. Liu, W. Feng, T. S. Yang, T. Yi, F. Y. Li, "Upconversion luminescence imaging of cells and small animals," *Nat. Protoc.* **8**(10), 2033–2044 (2013).
3. D. K. Chatterjee, A. J. Rufaihah, Y. Zhang, "Upconversion fluorescence imaging of cells and small animals using lanthanide doped nanocrystals," *Biomaterials* **29**(7), 937–943 (2008).
4. Y. I. Park, J. H. Kim, K. T. Lee, K. S. Jeon, H. B. Na, J. H. Yu, H. M. Kim, N. Lee, S. H. Choi *et al.*, "Nonblinking and nonbleaching upconverting nanoparticles as an optical imaging nanoprobe and T1 magnetic resonance imaging contrast agent," *Adv. Mate.* **21**(44), 4467–4471 (2009).
5. N. M. Idris, Z. Q. Li, L. Ye, E. K. W. Sim, R. Mahendran, C. L. Ho, Y. Zhang, "Tracking transplanted cells in live animal using upconversion fluorescent nanoparticles," *Biomaterials* **30**(28), 5104–5113 (2009).
6. C. Bouzigues, T. Gacoin, A. Alexandrou, "Biological applications of rare-earth based nanoparticles," *ACS Nano* **5**(11), 8488–8505 (2011).
7. M. Wang, C. C. Mi, W. X. Wang, C. H. Liu, Y. F. Wu, Z. R. Xu, C. B. Mao, S. K. Xu, "Immunolabeling and NIR-excited fluorescent imaging of HeLa cells by using NaYF4:Yb,Er upconversion nanoparticles," *ACS Nano* **3**(6), 1580–1586 (2009).
8. J. Hodak, Z. J. Chen, S. Wu, R. Etchenique, "Multiphoton excitation of upconverting

nanoparticles in pulsed regime," *Anal. Chem.* **88**(2), 1468–1475 (2016).
9. M. X. Yu, F. Y. Li, Z. G. Chen, H. Hu, C. Zhan, H. Yang, C. H. Huang, "Laser scanning up-conversion luminescence microscopy for imaging cells labeled with rare-earth nanophosphors," *Anal. Chem.* **81**(3), 930–935 (2009).
10. L. Y. Zeng, L. C. Xiang, W. Z. Ren, J. J. Zheng, T. H. Li, B. Chen, J. C. Zhang, C. W. Mao, A. G. Li, A. G. Wu, "Multifunctional photosensitizer-conjugated core–shell Fe3O4@NaYF4:Yb/Er nanocomplexes and their applications in T2-weighted magnetic resonance/upconversion luminescence imaging and photodynamic therapy of cancer cells," *RSC Adv.* **3**(33), 13915–13925 (2013).
11. L. Y. Zeng, L. J. Luo, Y. W. Pan, S. Luo, G. M. Lu, A. G. Wu, "In vivo targeted magnetic resonance imaging and visualized photodynamic therapy in deep-tissue cancers using folic acid-functionalized superparamagnetic-upconversion nanocomposites," *Nanoscale* **7**(19), 8946–8954 (2015).
12. E. Barkai, Y. J. Jung, R. Silbey, "Theory of single-molecule spectroscopy: Beyond the ensemble average," *Annu. Rev. Phys. Chem.* **55**(55), 457–507 (2004).
13. J. J. Zhou, S. Q. Xu, J. J. Zhang, J. R. Qiu, "Upconversion luminescence behavior of single nanoparticles," *Nanoscale* **7**(37), 15026–15036 (2015).
14. D. J. Gargas, E. M. Chan, A. D. Ostrowski, S. Aloni, M. V. P. Altoe, E. S. Barnard, B. Sanii, J. J. Urban, D. J. Milliron, B. E. Cohen, "Engineering bright sub-10-nm upconverting nanocrystals for single-molecule imaging," *Nat. Nanotechnol.* **9**(4), 300–305 (2014).
15. H. Li, Z. G. Gui, Y. Liang, Z. S. Yu, A. G. Wu, "Measurement of fluorescence life time of single up-conversion nanoparticle," *Opt. Precision Eng.* **25**(2), 319–324 (2017).
16. D. R. Gamelin, H. U. Gudel, *Upconversion Processes in Transition Metal and Rare Earth Metal Systems, Transition Metal and Rare Earth Compounds*, Springer, Germany (2001).